J. Med. Biol. Eng. (2017) 37:357–364
DOI 10.1007/s40846-017-0228-2

ORIGINAL ARTICLE

Integrating Compliant Actuator and Torque Limiter Mechanism for Safe Home-Based Upper-Limb Rehabilitation Device Design

Songyuan Zhang[1,2] · Shuxiang Guo[3,4] · Yili Fu[1] · Luc Boulardot[2] · Qiang Huang[3] · Hideyuki Hirata[4] · Hidenori Ishihara[4]

Received: 23 November 2015 / Accepted: 17 August 2016 / Published online: 24 March 2017

Abstract Stroke patients may prefer to rehabilitate at home, which limits their access to appropriate training devices and safety without supervised assistance by qualified personnel. However, most training devices are bulky and lack adequate safety for home-based training. To address this limitation, we have developed a device with a variable stiffness actuator (VSA) that was designed in the vsaUT-II and an effective torque limiter mechanism. First, compared with traditional actuators with very high mechanical impedance, actuators with adaptive compliance have many advantages for rehabilitation devices. For instance, compliant actuators can guarantee patient safety, especially, when a muscle spasm occurs. Moreover, stiffness can be adjusted to adapt to a specific level of patient impairment. Compliance in our device was realised using a VSA. Second, to avoid any danger in the absence of professionally supervised assistance, a novel torque limiter mechanism was designed. The mechanism can be released and effectively reduces the driving force whenever a spasm occurs. The experimental results prove that by adjusting the ratio between the internal springs and actuator output, the output stiffness is changed. The dynamic modeling of the device was also designed within a small deflection of the elastic elements. The torque limiter mechanism was evaluated with variable stiffness for ensuring safety in various conditions.

Keywords Home-based · Safety · Self-administered training · Compliant actuator · Torque limiter mechanism

1 Introduction

Stroke has become a leading cause of adult disability. Every year in the US, approximately 795,000 individuals experience a new or recurrent stroke [1]. Stroke can lead to impaired motor control of the upper and lower limbs with significant impairment of daily activities.

Traditional therapies help regain motor function but require one-to-one manual interaction, which is both labor intensive and expensive [2]. An effective and stable rehabilitation process can be offered by robot-mediated therapy [3]. Robot-mediated therapies for the upper limbs of stroke survivors began in the 1990s [4]. State-of-the-art therapeutic robots fit into one of the several categories such as endpoint manipulators [5, 6], cable suspensions [7] and power exoskeletons [8, 9]. Among them, exoskeletons have proved to be beneficial for the control and measurement of the angle or torque on each joint of an impaired limb, which is important for rehabilitation training [10]. In particular, Mao et al. designed lightweight exoskeletons for rehabilitation by replacing the rigid links with lightweight cuffs fixed to the moving limb segments of the human arm. Motor-driven cables are routed though these cuffs to move the limb segments that are relative to each other [11].

✉ Songyuan Zhang
s13d505@stmail.eng.kagawa-u.ac.jp

✉ Shuxiang Guo
guoshuxiang@bit.edu.cn

1 State Key Laboratory of Robotics and System, Harbin Institute of Technology, Harbin 150080, China

2 Graduate School of Engineering, Kagawa University, Takamatsu, Kagawa 761-0396, Japan

3 Key Laboratory of Convergence Medical Engineering System and Healthcare Technology, The Ministry of Industry and Information Technology, School of Life Science and Technology, Beijing Institute of Technology, Haidian District, Beijing 100081, China

4 Department of Intelligent Mechanical Systems Engineering, Kagawa University, Takamatsu, Kagawa 761-0396, Japan

Moreover, considering the inconvenience of regular travel to rehabilitation centers, patient demand for home-based rehabilitation is expected to increase. However, most of the latest reported training devices are not easily transportable or compact [12, 13]. Moreover, physical safety will likely be one of the issues associated with robotic devices, because robot-assisted training involves high human–machine interaction. This is especially true for a home-based device when a spasmodic event (involuntary contraction of a muscle or muscle group) occurs [14].

Active impedance control can be realised using a rigid actuator with closed-loop torque control. However, high inherent impedance beyond the control bandwidth can result in a dangerous situation [15]. Compared with conventional robots using “stiff actuation” and high levels of kinetic energy, compliance actuation is safer. Therefore, compliance actuation that allows deviation from its own equilibrium position would be beneficial while using rehabilitation robots. Such deviations depend on the applied external force and mechanical properties of the actuators [16, 17].

New actuators based on this principle such as the series elastic actuator (SEA) have been introduced into compliant robot design. Song et al. developed a portable exoskeleton device on the basis of a concept similar to SEAs [18]. The added compliance makes robots intrinsically safe and achieves energy-efficient actuation. SEA-based robotic devices enabled the generation of low impedance using a closed-loop interaction control modality [19]; however, SEAs have fixed compliance properties. As an improvement to compliant actuation, the concept of a variable stiffness actuator (VSA), which has adaptable compliance properties, was proposed [17]. VSAs also negotiate a trade-off between compliancy and accuracy, i.e., the compliance of VSAs can be adjusted for different tasks. For example, Lenzi et al. proposed the NEUROExos, which is a variable-impedance powered-elbow exoskeleton device [8]. An antagonistic actuation system provides software-controllable passive compliance. Variable stiffness is beneficial to the patient’s specific level of impairment [8].

Unlike these existing devices that are not transportable and do not have the safety features needed for unsupervised training, this paper describes the design of a training device that allows stroke patients to rehabilitate safely at home, without supervised assistance. We specifically designed a device that comprises a compliant variable stiffness actuator to ensure patient safety in the event of muscle spasm. We also designed a novel torque limiter mechanism to avoid danger in the absence of qualified personnel. Moreover, training strategies (passive or active training) can be selected for different patient conditions and recovery processes.

In this study, in detail, a compliant actuator-based exoskeleton device was designed for elbow joint training. The device can adjust output stiffness using an adjustable stiffness mechanism for patients with different levels of impairment. The actuator was designed on the basis of the vsaUT-II [20], and we applied its advantages to elbow joint training. When a high stiffness value is set, the device output can accurately track a pre-defined trajectory using a typical proportional-integral-derivative (PID) controller. If the stiffness is decreased, the limb’s weight will cause an error between the movement of the patient’s limb and pre-defined trajectory. Thus, the device can allow different error levels with respect to the desired trajectory. The importance of the stiffness variable was mentioned in a previous study, which reported that the variable compliance is a basic feature for a rehabilitation device to adapt to a specific level of impairment of the patient [14]. With a closed-loop interaction control strategy, the output impedance can also be adjusted for active training [19]. Considering that the compliant actuator may require a response time for adjusting to a safe stiffness range, a torque limiter mechanism was designed. The torque limiter can passively operate without a complex control algorithm and promptly react in dangerous situations.

2 Materials and Methods

2.1 Mechanical Design

The designed device can realise both passive and active self-administered training at home. During passive training, a programmed motion pattern is required because repetitive movement is the most effective approach for patients who cannot autonomously move [21]. However, a suitable impedance (resistive torque) provided by the device is beneficial to patients with limited motor functions [22]. In general, it is difficult to build a device that can realise both passive and active training when a large reduction gear is used, which causes non-backdrivability. The difficulty is due to the different functional requirements; compared with passive training, which requires high joint impedance, active training requires near-zero impedance [14]. However, without a large reduction gear, the device volume will be excessively large for home-based use. Because of the compliant actuator, the non-backdrivability problem can be resolved by a closed-loop interaction control method while ensuring adequately torque performance [18]. The other designed features of the proposed device are high safety and reliability.

Figure 1a shows a prototype of the proposed device configured for home-based rehabilitation training. A patient’s impaired forearm is fixed to an arm supporter

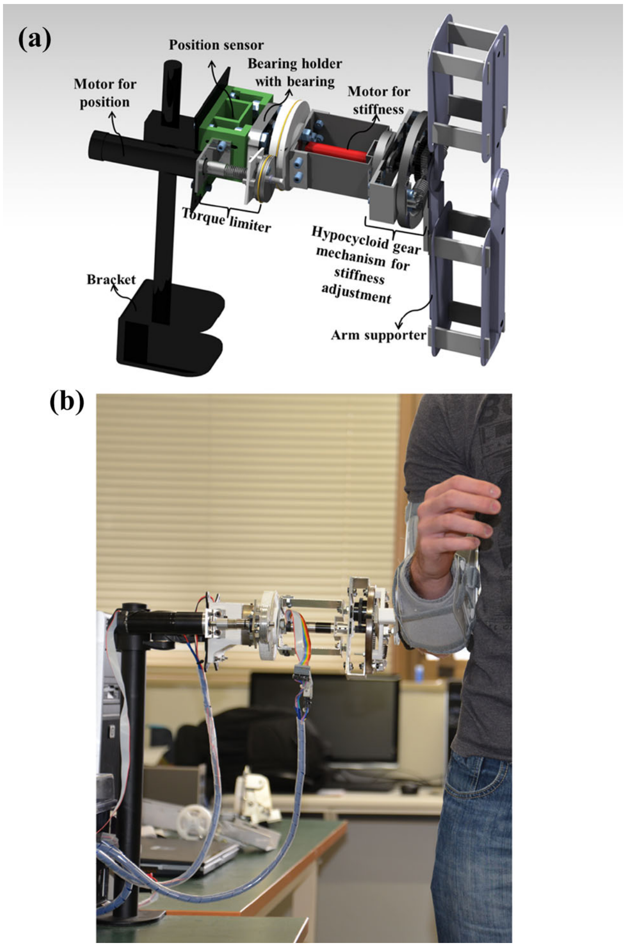

Fig. 1 **a** CAD drawing of the exoskeleton device prototype and **b** a user implementing training using this device

while the device performs the training as shown in Fig. 1b. The device is moveable and can be fixed to a solid table or wheelchair and adjusted for a comfortable posture. Main frame of the device is aluminum, and several connection parts were built using 3D-printing technology to reduce cost. Because of the actuator designed by Groothuis et al., the position control is independent of the stiffness control by means of two independent motors [23]. They also proved that by moving the pivot point along the lever arm, the involved forces can be minimised during stiffness change [23].

The actuator must ensure sufficient force/torque for performance of the training task while reducing the mass. Therefore, the flexion/extension motion is provided by a high-power-density Maxon motor (12 V, 60-W RE-30 DC motor, Switzerland) coupled to a Maxon GP32C planetary gearbox with a speed reduction ratio of 190:1. Power is transmitted to the turntable through a 1.0-mm diameter steel wire rope. The ratio between the torque limiter and turntable is 1:2. This type of force transmission can partly reduce friction compared with a gear mechanism. The rotation of the turntable causes the rotation of the device. One side of the turntable is connected to a bearing holder containing a low-friction bearing (BEM-6005ZZ; MIYOSHI, Japan). The device's rotary motion can be measured by a contactless Hall-IC angle sensor (CP-20HB, Midori Precisions Co., Ltd., Japan). An adjustable stiffness mechanism rotates together with the turntable and is used to adjust the mechanical stiffness. The detailed components are shown in Fig. 2. A Maxon motor (6 V, 8-W EC-max-16 DC motor, Switzerland) coupled to a Maxon GP16C planetary gearbox with a speed reduction ratio of 84:1 is used to adjust pivot position through a hypocycloid gear mechanism. Thus, the stiffness can be adjusted by changing the ratio between the internal springs and actuator output. The hypocycloid gear mechanism is designed with a special diameter so that the rotary motion can be converted to the pivot's linear motion [23]. Here a spring with a coefficient of 19.02 N/mm was selected.

Another important issue for the mechanical design of a home-based training device is safety. In particular, exoskeleton devices involve high human–machine interaction. A compliant actuator can detect a spasm and effectively reduce the interaction force [14]. However, a response time is still required, and a compliant actuator cannot provide a fast and reliable response. Any errors caused by the control algorithm will present a danger to the patient. Therefore, we designed a novel torque limiter mechanism that was added to the position driver, as shown in Fig. 3. The advantages of the torque limiter include high reliability without complex control algorithms and low cost. In detail, the coupling is used to connect the motor shaft and torque limiter. Four ball rollers are connected to a ball spline (BSSM6-150, Misumi, Japan), and the relative rotational motion with the axis is restricted. The clamp spring restricts the translational motion. The mechanism is similar to that of a clutch, in that

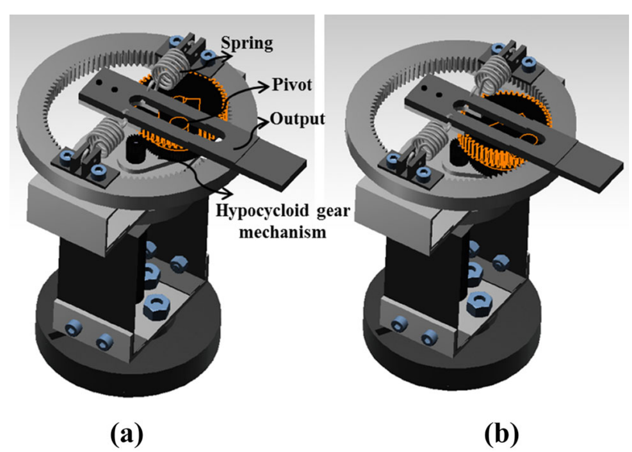

Fig. 2 Adjustable stiffness mechanism with hypocycloid gear mechanism. **a** and **b** show the different positions through which the pivot moves

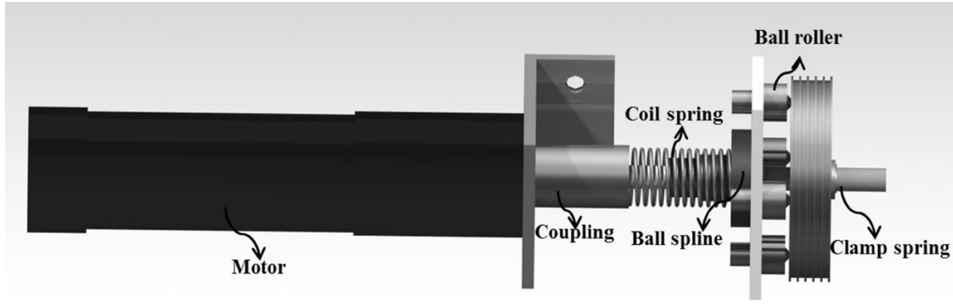

Fig. 3 CAD design for the torque limiter mechanism

the force of the compressed coil spring can push the four ball rollers into the fillister. When the external torque is larger than the threshold, the cable driver will rotate independent of the motor through the torque limiter mechanism. Thus, the device will rotate regardless of the motor position. The two situations in which the external torques are exceeded (or not) by the threshold are shown in Fig. 4. As Fig. 4a shows, the spring is compressed by the external torque and the balls are leaving the fillister. Conversely, Fig. 4b shows that the spring is not compressed; the motor can thus transfer the driving force through the torque limiter. Note that "not compressed" in Fig. 4b means not exceeding the preset threshold beyond the equilibrium position of the spring.

The torque limiter can operate automatically. Once the external torque reduces to a normal value, the cable driver will immediately provide the driving force. When the interaction force exceeds the preset threshold, the ball rollers will be away from the fillister due to further spring compression. This ensures patient safety when casual spasms occur. For different thresholds of the torque limiter, springs with different coefficients are selected. Here the spring coefficient was 7.5 N/mm for performance testing, although it can easily be changed as per patient status.

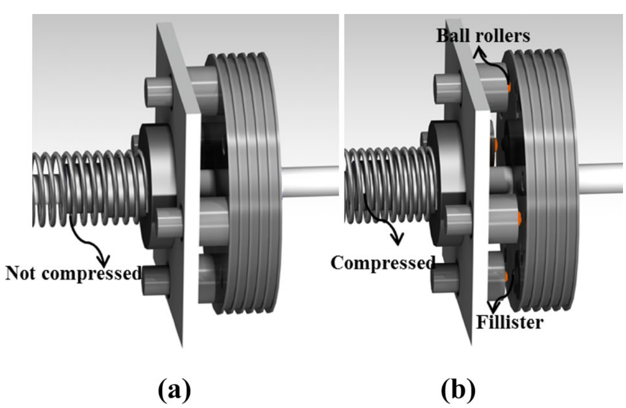

Fig. 4 **a** Ball rollers are entering holes in the cable driver. **b** Ball rollers are not entering holes in the cable driver

2.2 Control System Design

For the proposed device, there are two alternative control strategies for passive and active training. A typical PID algorithm was used for passive training position control, in which a pre-defined trajectory was programmed. The output stiffness was adjusted with open-loop control to vary pivot position. The torque limiter can passively operate without any control algorithm. A closed-loop interactive control method can be used to generate variable impedances for active training [24, 25]. Here we mainly focus on passive training, with variable stiffness for different impairment levels, and on functional evaluation of the torque limiter mechanism.

The control system used for the training device comprises two parts: a high-level control system (Windows 7 Professional system with a 3.0-GHz AMD processor and 4.0 GB RAM) and a low-level actuator control system (DSP 28335 processor inside the controller). The two systems communicate through a serial port. A user interface for the high-level control system was programmed in Visual C++ 2010 (Microsoft Co., Redmond, WA, USA). Thus, a control panel in the interface can be used for choosing training parameters and recording data for further teleassessment by therapists [26]. The teleassessment design used in this study can remotely determine the training parameters and recovery status.

2.3 Dynamic Modeling of the Compliant Actuator

The dynamic modeling of the variable stiffness part was performed, as illustrated in Fig. 5. The dynamic momentum of the output arm at point D is determined by Eqs. (1)–(3):

$$d = \left|\overrightarrow{OD}\right|, \tag{1}$$

$$L_{tot} = \left|\overrightarrow{O_2 I}\right|, \tag{2}$$

$$\overrightarrow{\delta^0_{2/D}} = \begin{bmatrix} 0 \\ 0 \\ \ddot{\theta}\left[C + M_2\left(-dL_{tot} - 2d\lambda + \lambda L_{tot} + d^2 + \lambda^2 + \left(\frac{L_{tot}}{2}\right)^2\right)\right] + \dot{\theta} M_2\left[-2d\dot{\lambda} + \dot{\lambda} L_{tot} - 2\lambda\dot{\lambda}\right] \end{bmatrix}, \tag{3}$$

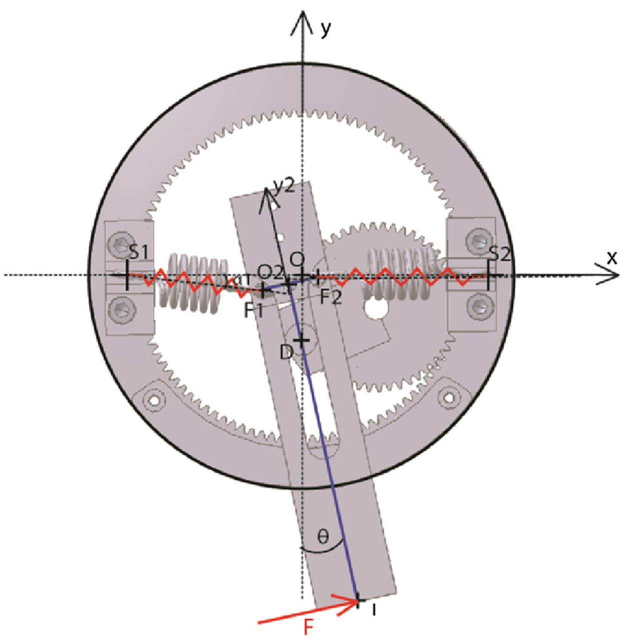

Fig. 5 Modeling for the compliant actuator

where θ is the rotation angle of the output arm around point D along the $\vec{z}$ axis, λ is the displacement of the output arm along the $\overrightarrow{y_2}$ axis, M_2 is the mass of the output arm, C is the inertial moment along the $\vec{z}$ axis and $\left|\overrightarrow{O_2G_2}\right| = \frac{L_{tot}}{2}$.

Here we consider that λ is negligible compared to the movement due to θ when the output deflection is small. Therefore, we assumed that $\lambda = 0, \dot{\lambda} = 0 \text{and} \ddot{\lambda} = 0$; therefore, the system can be simplified into

$$\overrightarrow{\delta^0_{2/D}} = \begin{bmatrix} 0 \\ 0 \\ \ddot{\theta}\left[C - M_2\left(2d^2 - \left(d - \frac{L_{tot}}{2}\right)^2\right)\right] \end{bmatrix}. \tag{4}$$

Because of the kinematics momentum theorem, Eqs. (5)–(8) can be respectively obtained as

$$\left(\sum moment\right)\vec{z} = \overrightarrow{\delta^0_{2/D}}\vec{z}, \tag{5}$$

$$\left(\sum moment\right)\vec{z} = \left(M_D\left(\overrightarrow{F_{s1}}\right) + M_D\left(\overrightarrow{F_{s2}}\right) + M_D(\vec{F})\right)\vec{z}, \tag{6}$$

$$M_D\left(\overrightarrow{F_{s1}}\right) + M_D\left(\overrightarrow{F_{s2}}\right) + M_D(\vec{F}) = \ddot{\theta}\left[C - M_2\left(2d^2 - \left(d - \frac{L_{tot}}{2}\right)^2\right)\right], \tag{7}$$

and

$$\ddot{\theta} = \frac{M_D\left(\overrightarrow{F_{s1}}\right) + M_D\left(\overrightarrow{F_{s2}}\right) + M_D(\vec{F})}{C + M_2\left(-d \cdot L_{tot} - d^2 + \left(\frac{L_{tot}}{2}\right)^2\right)}, \tag{8}$$

where $\overrightarrow{F_{s1}}$ and $\overrightarrow{F_{s2}}$ represent the force on springs 1 and 2, respectively. $|\vec{F}|$ varies with time and is perpendicular to the output arm. Moreover, $M_D(\vec{F}), M_D\left(\overrightarrow{F_{s1}}\right)$ and $M_D\left(\overrightarrow{F_{s2}}\right)$ represent the moments of forces $\vec{F}$, $\overrightarrow{F_{s1}}$, and $\overrightarrow{F_{s2}}$ on point D, respectively.

3 Results and Discussion

3.1 Simulation Results for the Compliant Actuator

The simulation results reflecting the relationship between the output deflection angle and generated force are shown in Fig. 6. We chose four stiffness levels by moving the pivot for 0, 5, 10 and 15 mm. The curves in Fig. 6 were not stable because the spring inertia was not considered. However, the instability had no influence on the trend between the deflection and force for varying stiffness.

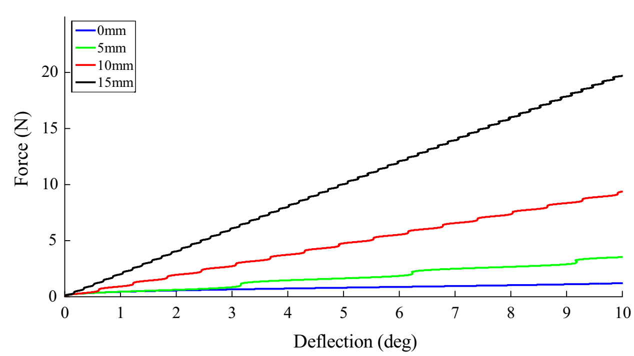

Fig. 6 Simulation results obtained via dynamic modeling

3.2 Static Characterization for the Compliant Actuator

As aforementioned, the stiffness is controlled by changing the ratio between the internal springs and actuator output. Thus, by controlling the pivot's moving position, the stiffness can be changed. An experiment was conducted for verifying the static characterization for stiffness control, as shown in Fig. 7. In this study, the static characterization is aimed at evaluating how device control can change joint stiffness and the influence on the static passive behavior of the joint. The similar method was also applied in [9]. A six-axis force sensor (MINI 4/20; BL AUTOTEC, LTD.) was fixed to a solid surface and attached to the output link 91 mm away from the center of rotation. The force perpendicular to the output was calculated as $\sqrt{F_x^2 + F_z^2}$. We manually rotated the frame clockwise, and an output deflection was caused by the springs. An inertial sensor (MTx sensor, Xsens, Enschede, the Netherlands) was installed on the output arm for measuring the output rotation angle. The rotation angle of the device frame was recorded by the sensor. The deflection, which is defined as the deviation of the output from its own equilibrium, was measured as the difference between the rotation angles of the output and frame. We selected four parameters (0, 5, 10 and 15 mm) to represent the distances that the pivot moves from the rotation center. The experimental results of static characterization are shown in Fig. 8. For each parameter, the procedure was repeated five times to obtain the error area. Data recorded through a force sensor was filtered by a low-pass Butterworth filter that had a cutoff frequency of 10 Hz. The experimental results plotted in Fig. 8 prove that by increasing the selected parameters, a higher slope of the force vs. deflection curve can be obtained. The mean values for each group were also calculated and are plotted in Fig. 8. Therefore, from the experimental results, the passive joint stiffness was increased by increasing the selected parameters. The joint stiffness for each parameter (0, 5, 10 and 15 mm) was estimated using a linear fitting method; the results of these estimations, along with those obtained via the RMSE are listed in Table 1. By comparing the results with the simulation results plotted in Fig. 6, it was found that the results do not exactly correspond. The error was because the friction and displacement of the output (λ) were not considered in the simulation results. During actual training, the deflection will not be excessively large; therefore, the displacement of the output (λ) can be ignored in the simulated case. Moreover, from the experimental results, it can be seen that a large deflection may cause a displacement of the output (λ) and that the force vs. deflection curve may not be linear.

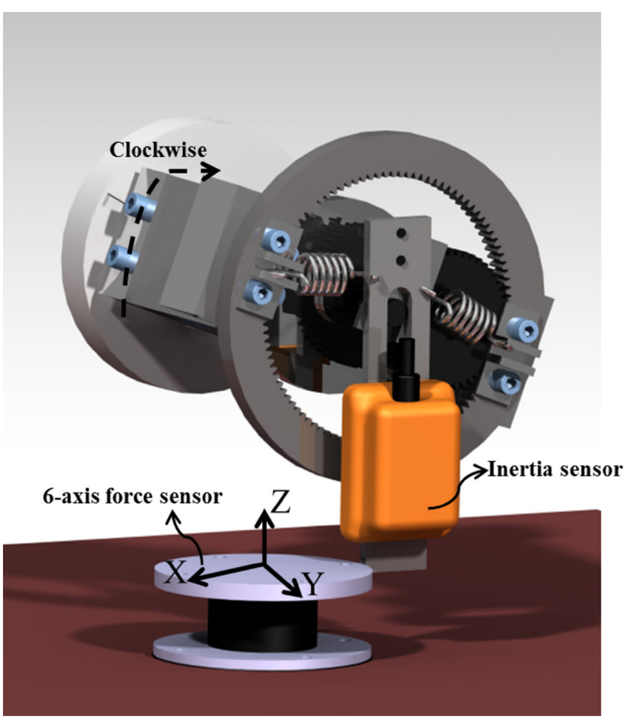

Fig. 7 Experimental setup for the static characterization

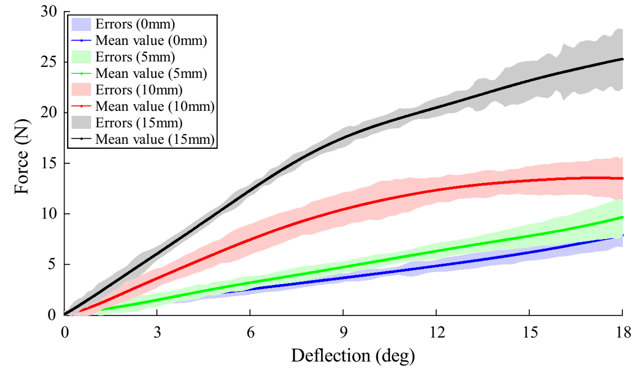

Fig. 8 Experimental results with varying stiffness

During rehabilitation training, a suitable stiffness can be selected for a better recovery of patient impairment. The compliance can also protect patients from danger when spasms occur.

3.3 Evaluation of the Torque Limiter Mechanism

As aforementioned, a spasm is an involuntary contraction of muscles. A large interaction force will be generated by a spasm, which may be dangerous to the patient. The torque

Table 1 Estimated stiffness for each parameter

Moving distance (mm)	0	5	10	15
k (N/°)	0.38	0.53	1.18	1.95
RMSE (Nmm)	0.43	0.71	2.50	3.31

limiter mechanism can make the cable driver rotate independently from the output when a spasm occurs. The interaction force between the patient and device can thus be decreased. The maximum torque of the torque limiter mechanism can be calculated by

$$\tau_{\max} = \left[F_{spring} + k(L_{\max} - L)\right]L_1 \tan^{-1}\left(A \sin\left(\frac{\frac{d}{2} - L}{\frac{d}{2}}\right)\right), \tag{9}$$

where $\tau_{\max}$ represents the maximum torque before entering free mode (where the external torque is larger than the threshold), F_{spring} is the force generated by the spring when the ball rollers are in the fillister (Fig. 4), L_1 is the distance of the ball rollers from the center of rotation, d is the diameter of the balls and L is the depth of the ball rollers in the fillister.

The torque limiter mechanism can passively operate without a complex control algorithm, which induces a quick and stable response. The stiffness may cause a deflection of the output; therefore, it is necessary to evaluate the performance of the torque limiter mechanism with variable stiffness. During actual training, if the interaction force caused by a spasm is not excessively large, the compliance itself can ensure patient safety.

The experimental setup was the same as that shown in Fig. 7. The only difference is that the device output was programmed to rotate clockwise with an angular frequency of 1 Hz until blocked by the force sensor. Three levels of stiffness were adjusted for the 0, 10 and 20 mm that the pivot moved from the rotation center. Due to compliance, the output is blocked by the force sensor and will have a minor deflection at first. Once the force exceeds the threshold of the torque limiter mechanism, the output arm will be detached from the cable driver. The MTx sensor (static accuracy for roll/pitch <0.5°, angular resolution: 0.05°) was used to record the rotational angle of the turntable, and the force sensor measured the interaction force [27].

The experimental results are plotted in Figs. 9 and 10. In Fig. 9, it is observed that there are two states. For state (a), the output arm is driven by the cable driver. However, for state (b), the device is in free mode. After the output is blocked it will be detached, although the motor continues to rotate (see Fig. 9). The lag that the device displays in free mode is different from the output stiffness. The position data alone cannot adequately explain the performance. Therefore, the interaction force was recorded and synchronously plotted in Fig. 10. This figure also proves that after the device enters into the free mode, the force becomes small, which will sufficiently ensure patient safety. Outputs with higher stiffness will enter into the free mode before outputs with lower stiffness.

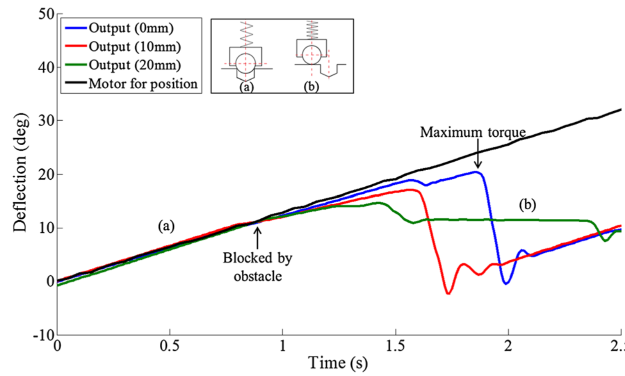

Fig. 9 Postion data for the torque limiter mechanism

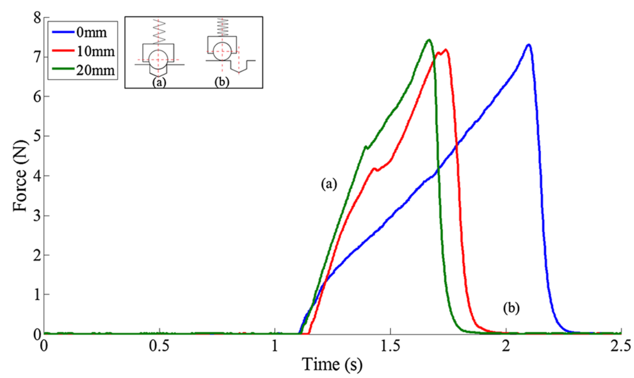

Fig. 10 Interaction force for the torque limiter mechanism

4 Conclusion

Safe home-based rehabilitation is expected to create increased demand because of the inconvenience of travelling to rehabilitation centers. However, the demand is still limited by the lack of a suitable training device. In this study, we propose a light-weight, low-cost exoskeleton device with a compliant actuator and torque limiter mechanism for safe home training. Muscle spasms may be dangerous, especially, with exoskeleton devices that are closely attached to the forearm. Both a compliant actuator and novel torque limiter mechanism were applied here for ensuring safety when spasm occurs. For ensuring sufficient output performance while reducing the total weight, an actuator with a large reduction gear was applied, which induced non-backdrivability. For more active training, the non-backdrivability problem can be solved by a closed-loop interaction control method combined with the compliant actuator design.

In this paper, dynamic modeling of the compliant actuator was done with minor deflections. The displacement of the output (λ) was ignored for the modeling. Considering that in an actual situation friction may have an influence on the simulation results, an experiment was conducted to evaluate force vs. deflection. Force vs. deflection with a large deflection was also considered, although this case may not happen in actual training. Subsequently, the performance of the torque limiter mechanism was also evaluated with variable stiffness. The experimental results prove the safety of the device with the mechanism. By combining the compliant actuator and torque limiter mechanism, although there will be a reaction time in which the device changes to low stiffness when a spasm occurs, the torque limiter can also ensure a force not larger than a pre-defined value for each individual.

Acknowledgements This research is partly supported by National Natural Science Foundation of China (61375094), Key Research Program of the National Science Foundation of Tianjin (13JCZDJC26200), National High Tech. Research and Development Program of China (No. 2015AA043202) and JSPS KAKENHI Grant Number 15K2120.

References

1. Lloyd-Jones, D., Adams, R. J., Brown, T. M., Carnethon, M., Dai, S., De Simone, G., et al. (2010). Heart disease and stroke statistics–2010 update: A report from the American Heart Association. *Circulation, 121,* 46–215.
2. Langhorne, P., Coupar, F., & Pollock, A. (2009). Motor recovery after stroke: A systematic review. *The Lancet Neurology, 8*(741–754), 2009.
3. Novak, D., Nagle, A., Keller, U., & Riener, R. (2014). Increasing motivation in robot-aided arm rehabilitation with competitive and cooperative gameplay. *Journal of NeuroEngineering and Rehabilitation, 11*(1), 64.
4. Basteris, A., Nijenhuis, S. M., Stienen, A. H., Buurke, J. H., Prange, G. B., & Amirabdollahian, F. (2014). Training modalities in robot-mediated upper limb rehabilitation in stroke: a framework for classification based on a systematic review. *Journal of NeuroEngineering and Rehabilitation, 11*(1), 111.
5. Hogan, N., Krebs, H. I., Sharon, A., & Chammarong, J. (1995). *Interactive robotic therapist*. U.S. Patent, 5,466,213, 14.
6. Song, Z., Guo, S., & Fu, Y. (2011). Development of an upper extremity motor function rehabilitation system and assessment system. *Int. J. Mechatron. Autom., 1*(3/4), 19–28.
7. Mayhew, D., Bachrach, B., Rymer, W. Z., & Beer, R. F. (2005). Development of the MACARM-a novel cable robot for upper limb neurorehabilitation. In: *Proceedings of the 9th international conference on rehabilitation robotics*, pp. 299–302.
8. Vitiello, N., Lenzi, T., Roccella, S., Rossi, S. M. M. D., Cattin, E., Giovacchini, F., et al. (2013). NEUROExos: A powered elbow exoskeleton for physical rehabilitation. *IEEE Transactions on Robotics, 29*(1), 220–235.
9. Wang, W., Tsai, B., Hsu, L., Fu, L., & Lai, J. (2014). Guidance-control-based exoskeleton rehabilitation robot for upper limbs: Application to circle drawing for physiotherapy and training. *Journal of Medical and Biological Engineering, 34*(3), 284–292.
10. Stienen, A. H. A., Hekman, E. E. G., van der Helm, F. C. T., & van der Kooij, H. (2009). Self-aligning exoskeleton axes through decoupling of joint rotations and translations. *IEEE Transactions on Robotics, 25*(3), 628–633.
11. Mao, Y., & Agrawal, S. K. (2012). Design of a cable-driven arm exoskeleton (CAREX) for neural rehabilitation. *IEEE Transactions on Robotics, 28*(4), 922–931.
12. Nijenhuis, S. M., Prange, G. B., Amirabdollahian, F., Sale, P., Infarinato, F., Nasr, N., et al. (2015). Feasibility study into self-administered training at home using an arm and hand device with motivational gaming environment in chronic stroke. *Journal of NeuroEngineering and Rehabilitation, 12,* 89.
13. Sivan, M., Gallagher, J., Makower, S., Keeling, D., Bhakta, B., O'Connor, R. J., et al. (2014). Home-based computer assisted arm rehabilitation (hCAAR) robotic device for upper limb exercise after stroke: Result of a feasibility study in home setting. *Journal of NeuroEngineering and Rehabilitation, 11,* 163.
14. Lenzi, T., Vitiello, N., De Rossi, S. M. M., Roccella, S., Vecchi, F., Carrozza, M. C. (2011). NEUROExos: A variable impedance powered elbow exoskeleton. In *Proceeding of 2011 IEEE international conference on robotics and automation*, pp. 1419–1426.
15. Rocon, E., Belda-Lois, J. M., Ruiz, A. F., Manto, M., Noreno, J. C., & Pons, J. L. (2007). Design and validation of a rehabilitation robotic exoskeleton for tremor assessment and suppression. *IEEE Transactions Neural Systems and Rehabilitation Engineering, 15*(3), 367–378.
16. Ham, R. V., Sugar, T. G., Vanderborght, B., Hollander, K. W., & Lefeber, D. (2009). Compliant actuator designs. *IEEE Robotics and Automation Magazine, 16*(3), 81–94.
17. Vanderborght, B., Albu-Schaeffer, A., Bicchib, A., Burdetd, E., Caldwelle, D. G., Carlonic, R., et al. (2013). Variable impedance actuators: A review. *Robotics and Autonomous Systems, 61*(12), 1601–1614.
18. Song, Z., Guo, S., Pang, M., Zhang, S., Xiao, N., Gao, B., et al. (2014). Implementation of resistance training using an upper-limb exoskeleton rehabilitation device in elbow joint. *Journal of Medical and Biological Engineering (JMBE), 34*(2), 188–196.
19. Pratt, G. A., & Williamson, M. M. (1995). Series elastic actuator. In *Proceedings of IEEE/RSJ international conference on intelligent robots and systems*, pp. 399–406, Pittsburgh.
20. Groothuis, S. S., Rusticelli, G., Zucchelli, A., Stramigioli, S., & Carloni, R. (2012). The vsaUT-II: A novel rotational variable stiffness actuator. *IEEE International Conference on Robotics and Automation (ICRA), 2012,* 3355–3360.
21. Oblak, J., Cikajlo, I., & Matjacic, Z. (2010). Univesral haptic drive: A robot for arm and wrist rehabilitation. *IEEE Transactions Neural Systems and Rehabilitation Engineering, 18*(3), 293–302.
22. Rahman, T., Sample, W., Jayakumar, S., King, M. M., Wee, J. Y., Seliktar, R., et al. (2006). Passive exoskeleton for assisting limb movement. *Journal of Rehabilitation Research and Development, 43*(5), 583–590.
23. Groothuis, S. S., Rusticelli, G., Zucchelli, A., Stramigioli, S., & Carloni, R. (2014). The variable stiffness actuator vsaUT-II: Mechanical design, modeling, and identification. *IEEE/ASME Transactions on Mechatronics, 91*(2), 589–597.
24. Zhang, S., Guo, S., Gao, B., Hirata, H., & Ishihara, H. (2015). Design a novel telerehabilitation system with a force-sensing mechanism. *Sensors, 15*(5), 11511–11527.
25. Song, Z., & Guo, S. (2012). Design process of exoskeleton rehabilitation device and implementation of bilateral upper limb motor movement. *Journal of Medical and Biological Engineering, 32*(5), 323–330.
26. Zhang, S., Guo, S., Gao, B., Huang, Q., Pang, M., Hirata, H., et al. (2016). Muscle strength assessment system using sEMG-based force prediction method for wrist joint. *Journal of Medical and Biological Engineering, 36*(1), 121–131.
27. https://www.xsens.com/products/mtx/.